SAND93-3922

Flow Regime and Heat Transfer Models of IFCI 6.0

R. C. Schmidt and M. F. Young
Sandia National Laboratories,
Albuquerque, New Mexico

DRAFT FOR REVIEW

Report prepared for the
United States Nuclear Regulatory Commission
Office of Nuclear Regulatory Research

July 31, 1995

ABSTRACT

The Integrated Fuel-Coolant Interaction Code (IFCI) is a best-estimate computer program for analysis of phenomena related to mixing of molten nuclear reactor core material with reactor coolant (water). The stand-alone version of the code, IFCI 6.0, has been designed for analysis of small- and intermediate-scale experiments in order to gain insight into the physics (including scaling effects) of molten fuel-coolant interactions (FCIs), and to assess and validate the code's methods, models, and correlations..

In this report the flow regime and heat transfer models used in the current version of IFCI (IFCI 6.0) are described.

TABLE OF CONTENTS

Page

1. INTRODUCTION AND OVERVIEW

The **I**ntegrated **F**uel-**C**oolant **I**nteraction (IFCI) code is a 3-field compressible hydrodynamic code designed to model the mixing of molten nuclear reactor materials with reactor coolant (water). It is designed to handle, with varying degrees of empiricism, the four stages of fuel-coolant interactions: coarse mixing, triggering, detonation propagation, and hydrodynamic expansion. IFCI is under development at Sandia National Laboratories (SNL), and is sponsored by the United States Nuclear Regulatory Commission, Office of Nuclear Regulatory Research (USNRC/RES).

IFCI contains models for boiling rates, flow regimes, dynamic melt fragmentation, surface tracking, subcooling effects, melt oxidation, triggering, and propagation of the shock. These phenomena are essential to the modeling of fuel/coolant interactions. Relatively brief descriptions of many of these models have been provided in earlier reports [1,2]. In addition, a fairly detailed description of the models for melt fragmentation and droplet break-up is given in Reference [3]. The purpose of this report is to provide a detailed description of the flow regime and heat transfer models that are used in IFCI 6.0.

Section 2 provides a synopsis of the hydrodynamic fluids model and the governing conservation equations that provide that framework for all of the IFCI models. Section 3 describes the two phase (vapor-water) flow regime maps that are used in IFCI. These have been adopted primarily from TRAC [4,5] and MELPROG [6,7], and include both vertical and a horizontal flow regime maps. In Section 4, interfield heat transfer models are described in detail. These include the heat transfer between vapor and steam (Section 4.1), and between the melt and the vapor and steam (Section 4.2).

2. THREE-FIELD HYDRODYNAMIC FLUIDS MODEL

The IFCI hydrodynamic fluids model has been developed from the two-dimensional, four-field hydrodynamics model implimented in MELPROG [6,7] and uses MELPROG FLUIDS module hydrodynamics subroutines extensively. Furthermore, IFCI drivers, input and output routines were derived from MELPROG subroutines. The MELPROG hydrodynamics model was designed to treat up to four fields; (1) vapor (steam and H_2), (2) water, (3) debris, and (4) melt (in MELPROG, these are referred to as fields 1, 2, 3, and 4 respectively). Therefore, it is usually referred to as a four-field hydrodynamics model. In practice, however, MELPROG's fluid fields for solid debris ("field 3") and melt ("field 4") were <u>not</u> coupled because the required modeling information needed to separate fields 3 and 4 was deemed inadequate, and all corium, regardless of solid-liquid state, was placed in field 3, leaving the forth field inactive. In other words, MELPROG was always run with the fields for vapor, water, and debris "on," and the melt field was "off." (Note for clarity that MELPROG did have a seperate candling model in the CORE module to treat the relocation of molten core structure material.) In contrast, IFCI is always run with the steam, water, and melt fields "on," and the debris field is "off." As MELPROG did with field 3, all corium treated by IFCI, regardless of solid-liquid state, is placed in field 4, but the inter-field coupling terms with field 4 are uniquely IFCI models, not MELPROG models. Therefore, strictly speaking, IFCI uses a three-field hydrodynamics model, even though previous documentation has often referred to the model is a four-field model (with one field inactive).

2.1 Field Equations

The equation set used in IFCI is a three-field, two-dimensional, cylindrical geometry version of a set commonly used in multifield computational hydrodynamics and originally derived from the general field equations of Ishii [8,9]. A "field" in the context of multifield hydrodynamics is represented by separate momentum, mass continuity, and energy equations for each type and phase of material in the interaction. These three equations are solved for each "field." Mass, energy, and momentum transfer between fields are represented by coupling terms in the field equations for which constitutive relations must be provided. Also necessary is an equation of state for each field. Use of a multifield method with separate mass, momentum, and energy equations for each field allows slip between the various materials (vapor, coolant, and melt), and a different temperature for each material. The field equations, associated constitutive relations, equations of state, and initial and boundary conditions, are solved in IFCI by use of the SETS method developed by Mahaffy [10].

The basic conservation equations used in IFCI for each field "k" are given below in Equations 2.1 through 2.4. Values of k equal to 1, 2, and 3 denote the vapor, water, and melt fields respectively. Whenever a summation is used to indicate various interfield terms, the subscript j is also used to refer to the different fields and a double subscript is employed. These terms are for j and k except j=k.

Mass Conservation:

$$\frac{\partial}{\partial t}(\alpha_k \rho_k) + \nabla\bullet(\alpha_k \rho_k \vec{V}_k) - \sum_{j=1}^{3} \Gamma_{jk} - \Gamma_k = 0 \qquad (2.1)$$

Axial Momentum:

$$\frac{\partial}{\partial t} W_k + \vec{V}_k \bullet \nabla W_k + \frac{1}{\rho_k}\frac{\partial P}{\partial z} + \frac{1}{(\alpha\rho)_k}\sum_{j=1}^{3} Cz_{jk}(W_k - W_j)|W_k - W_j| + \frac{1}{(\alpha\rho)_k} Dz_k W_k |W_k| + F^v_{Zk} + g = 0 \qquad (2.2)$$

Radial Momentum:

$$\frac{\partial}{\partial t} U_k + \vec{V}_k \bullet \nabla U_k + \frac{1}{\rho_k}\frac{\partial P}{\partial r} + \frac{1}{(\alpha\rho)_k}\sum_{j=1}^{3} C_{Rjk}(U_k - U_j)|U_k - U_j| + \frac{1}{(\alpha\rho)_k} D_{Rk} U_k |U_k| + F^v_{Rk} = 0 \qquad (2.3)$$

Energy:

$$\frac{\partial}{\partial t}(\alpha_k \rho_k e_k) + \nabla\bullet(\alpha_k \rho_k e_k \vec{V}_1) + P\left[\frac{\partial \alpha_k}{\partial t} + \nabla\bullet \alpha_k \vec{V}_k\right] - \sum_{j=1}^{3} \Gamma_{jk} H_{sk} - \sum_{j=1}^{3} Q_{jk} - Q_{wk} - Q_{sk} = 0 \qquad (2.4)$$

In addition, a constraint on the sum of the fluid volume fractions is also required. By definition these volume fractions must always add to one, thereby satisfying the following equation:

$$1 - \alpha_s - \sum_{k=1}^{3} \alpha_k = 0 \qquad (2.5)$$

The virtual mass terms F^v_{Zk} and F^v_{Rk} appearing in Equations (2.2) and (2.3) are used to add stability to the multifield equations. The form used in IFCI is simplified from the full virtual mass expression as suggested in Bohl et al. [11] and is applied only to discrete vapor flows (i.e., k=1).

The expressions used in IFCI for the virtual mass terms can be written as follows.

$$F^v_{Zk} = \alpha_k \bar{\rho}_L C_{vm} \left[\frac{\partial}{\partial t} W_k - \bar{\alpha}_2 \frac{\partial}{\partial t} W_2 - \bar{\alpha}_3 \frac{\partial}{\partial t} W_3 \right] \tag{2.6}$$

$$F^v_{Rk} = \alpha_k \bar{\rho}_L C_{vm} \left[\frac{\partial}{\partial t} U_k - \bar{\alpha}_2 \frac{\partial}{\partial t} U_2 - \bar{\alpha}_3 \frac{\partial}{\partial t} U_3 \right] \tag{2.7}$$

In Equations (2.6) and (2.7), $\bar{\rho}_L$ is an effective liquid density for the water, melt and solid fields, $\bar{\alpha}_2$ is a normalized liquid field volume fraction, and the virtual mass coefficient, C_{vm}, is set to a value giving stability to the equation set [12],

$$C_{vm} = 4 \sqrt{\bar{\alpha}_1^{\,3} \, \bar{\alpha}_L \, \rho_1 / \bar{\rho}_L} \tag{2.8}$$

In Equations 2.1 through 2.5, α_k is the volume fraction with respect to the total finite difference-mesh cell volume. There can also be a non-flow volume fraction in the cell, as structures, α_s. The velocity vector $\vec{V}_k$ is composed of axial and radial components W_k and U_k. The third and fourth terms in Equation (2.1) represent mass transfer among the fields and external mass source terms, respectively. The mass transfer between steam and liquid water is treated implicitly in temperature and pressure, while the other mass transfers are explicit sources. In the momentum equations, the fourth term represents momentum transfer between the fields, the fifth term represents wall friction, and the sixth term is the virtual mass force described above. The coefficients, Cz_{jk} and $C_{R_{jk}}$, are evaluated explicitly based on the local flow regime. In the energy equation [see Equation (2.4)], the third term is the work term. The fourth term represents energy exchange between the fields due to phase change, with H_{sk} representing the saturation enthalpy. The fifth term represents heat transfer between fields. The sixth term represents external energy sources, and the seventh term is energy transfer to an interface at saturation.

Because there are three fields being treated, Equations (2.1) through (2.5) constitute a set of thirteen coupled, non-linear, partial differential equations that, along with material equations of state and constitutive relations for mass, energy and momentum exchange, form the hydrodynamic equation set of IFCI.

3. FLOW REGIME MODELS

3.1 Vertical Flow Regime Map

Shown in Figure 3-1 is the vertical flow map used in IFCI as the basis for calculating Cz_{12}. Also shown is the flow regime map used in TRAC[5]. In TRAC, a mass flow rate dependence for bubbly and slug flow is used, whereas in IFCI, this dependence has been neglected. However, this simplification only has impact when $0.3 < \alpha_v' < 0.5$ at mass flow rates above 2000 kg/(sec m^2).

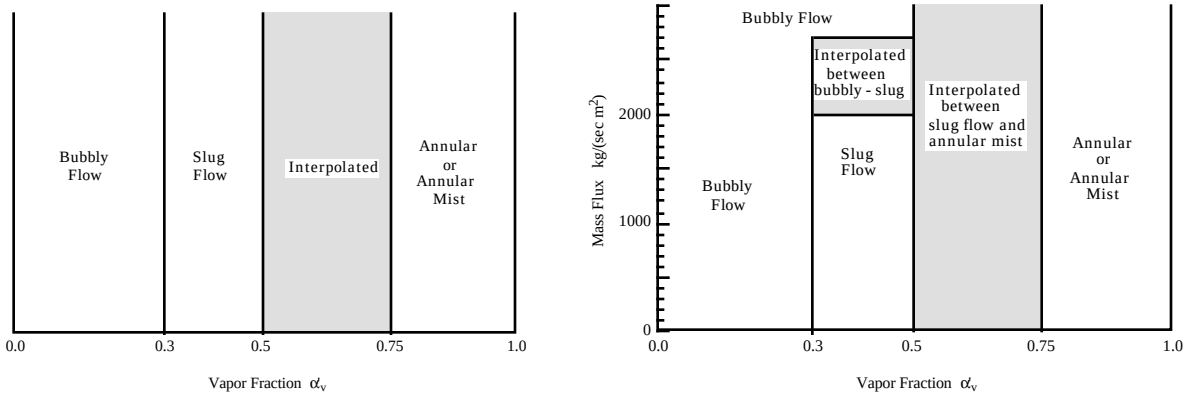

a. IFCI b. TRAC

Figure 3-1 A Comparison of the IFCI Vertical Water-Vapor Flow Regime Map with the TRAC Flow Regime Map

The IFCI vertical flow map depends only upon the normalized vapor volume fraction, α_v', to determine flow regime changes. The normalized fraction is defined as

$$\alpha_v' = \frac{\alpha_1}{(\alpha_1 + \alpha_2)} \tag{3.1}$$

The flow regime is bubbly flow when the normalized vapor volume fraction is less than 0.3 in a flow situation. The flow regime is slug, or bubbles growing to the size of the hydraulic diameter in the range from 0.3 to 0.5. Above 0.75, the regime is annular mist flow, where the water is in droplet form and the vapor is the continuous phase. The region from 0.5 to 0.75 is

a transition region between the slug and annular mist flows where interfacial values are determined by a smooth interpolation from one regime to the other.

3.2 Horizontal Flow Regime Map

In most applications of interest, vertical flow is dominant. However, a horizontal flow map is sometimes needed (especially when the water level in a cell must be determined). The flow map of Baker [13] is used as the basis for the horizontal steam-water flow map used in IFCI. IFCI uses a modified version of the map delineating 3 flow patterns. Both of these maps are based on corrected vapor and water mass fluxes, G_V' and G_L', respectively, that are given by:

$$G_V' = \frac{G_V}{\lambda} , \qquad G_L' = G_L \psi \tag{3.2}$$

where the factors λ and ψ are used to adjust for different water and vapor properties, as the original map is for air-water flows. These factors are defined as:

$$\lambda = \left(\frac{\rho_V}{\rho_A} \frac{\rho_L}{\rho_W} \right)^{1/2} , \qquad \psi = \left(\frac{\sigma_W}{\sigma} \right) \left\{ \frac{\mu_L}{\mu_W} \left(\frac{\rho_W}{\rho_L} \right)^2 \right\} \tag{3.3}$$

where

ρ_x = density of x, where x is v (vapor) or L (liquid water) (kg/m^3),
ρ_A = density of air at STP (kg/m^3),
ρ_W = density of water at STP (kg/m^3),
μ_L = viscosity of water (Pa-s),
μ_W = viscosity of water at STP (Pa-s),
σ = surface tension (Pa-m), and
σ_W = surface tension of water at STP (Pa-m).

These flow maps are shown in Figure 3-2 where the IFCI regions are superimposed over the flow regimes as proposed by Baker. The flow regime is bubbly flow whenever the the corrected water mass flux is greater than 2000. When the flux is below 2000, the flow regime is an annular mist or droplet flow if the corrected vapor flux is greater than 4.0 and stratified flow in the low vapor flow regimes.

The factors λ and ψ actually used in IFCI are calculated from polynomial fits to curves of λ and ψ for steam-water systems versus pressure given in Collier [14]. These are shown in Figure 3-3 and are given in Equations (3.4) and (3.5) using the S.I. units employed in IFCI.

$$\Psi = 0.678676 + 2.3526 \times 10^{-7} * P - 2.618 \times 10^{-14} * P^2 + 3.0491 \times 10^{-21} * P^3 \quad (3.4)$$

$$\lambda = \begin{cases} 1.0 + 5.7971 \times 10^{-7} * (P - 1.0 \times 10^5) & , \quad P > 7.0 \text{ MPa} \\ 5.0 + 2.2200 \times 10^{-7} * (P - 7.0 \times 10^6) & , \quad P > 7.0 \text{ MPa} \end{cases} \quad (3.5)$$

where "P" is the pressure in Pa.

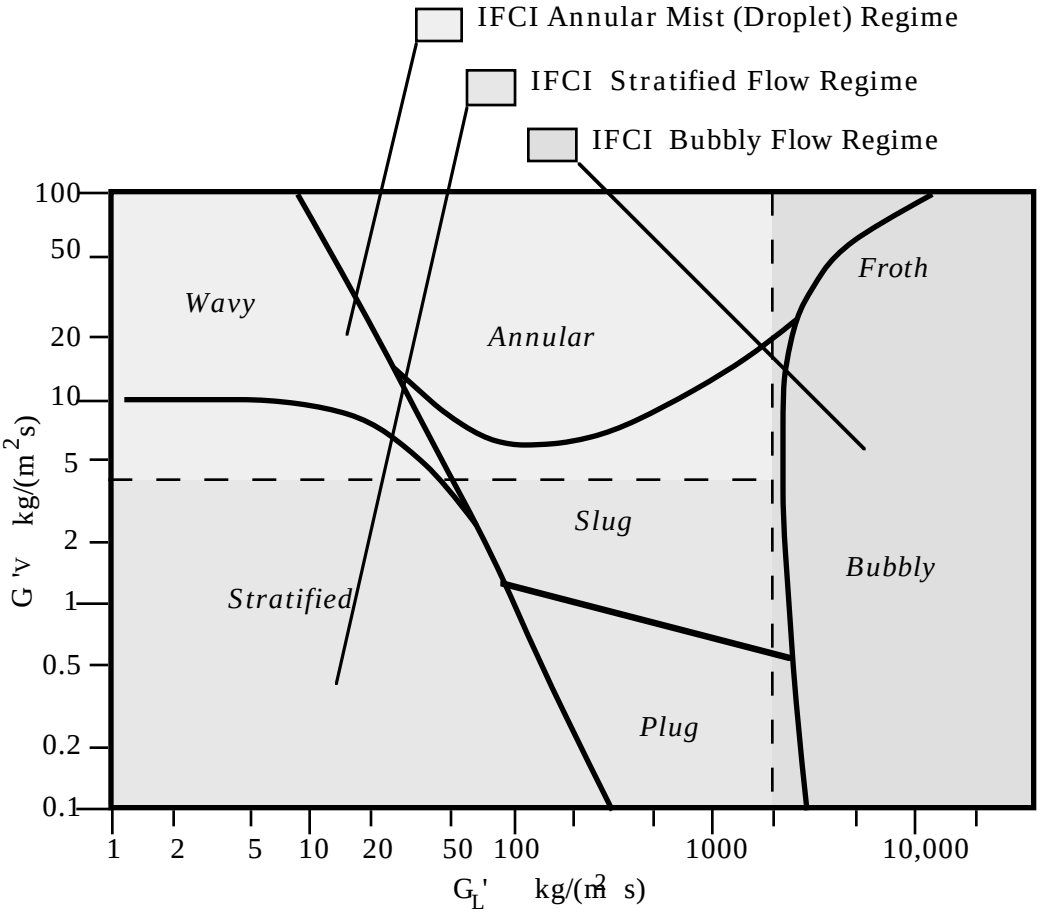

Figure 3-2 Flow-Regime Map for Two-Phase Horizontal Flow used in IFCI Compared to the Map of Baker [13].

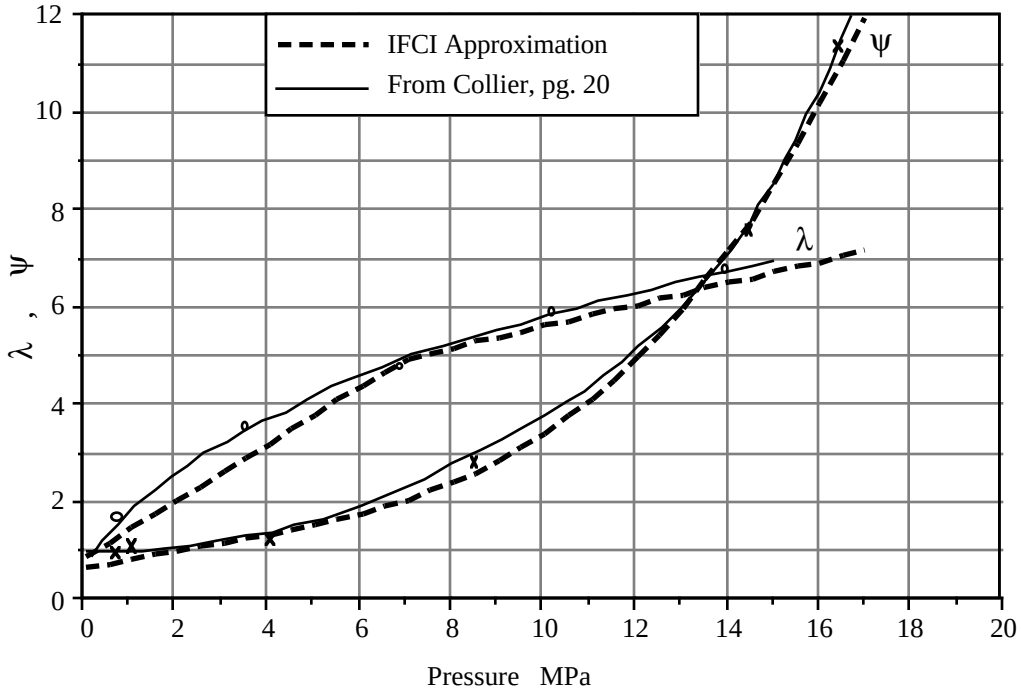

Figure 3-3 Comparison of the IFCI Approximation for λ and Ψ with the Data Given in Collier [14]

4. INTER-FIELD HEAT TRANSFER MODELS

As previously introduced, a conservation of energy equation (Equation (2.4)) is solved for each fluid field. Of interest in this section is the fifth term in this equation - the heat transfer that can occur between different fluid fields existing together in the same local region (i.e., control volume).

4.1 Heat Transfer Between Vapor (Field 1) and Water (Field 2)

The two-phase (steam/H_2 - liquid water) interfacial heat transfer models used in IFCI are primarily adopted from the TRAC-PF1/MOD1 computer code [5]. However, some adaptations or modifications have been implemented in IFCI. The use of these heat transfer correlations is tied to the simplified two-phase flow regime maps described above in Section 3.

Four regimes are defined in the vertical flow regime map. Which regime the fluids are in depends on the value of the normalized vapor volume fraction (or "void fraction"), α_v'. The flow regime is "bubbly flow" when the normalized volume fraction is less than 0.3. The flow regime is "slug flow" - or bubbles growing to the size of the hydraulic diameter - in the range from 0.3 to 0.5. Above 0.75, the regime is "mist" or "annular mist" flow, where the water is in droplet form and the vapor is the continuous phase. The region from 0.5 to 0.75 is a transition region between the slug and annular mist flows where interfacial values are determined by a smooth interpolation from one regime to the other. In Sections 4.1.2 through 4.1.5, the models and correlations applied for each of the four vertical flow regimes will be described.

In most applications of interest, vertical flow is dominant. However, a horizontal flow map is sometimes needed (especially when the water level in a cell must be determined). The flow map of Baker [13] is used as the basis for the horizontal steam-water flow map used in IFCI. As explained in Section 3.2, IFCI uses a modified version of the horizontal flow map of Baker delineating 3 flow patterns. In Sections 4.1.6 through 4.1.8, the models and correlations applied for each of the three vertical flow regimes will be described.

Because the flow is not always dominantly one direction or the other, a means for interpolating between the horizontal and vertical flow regimes has been implemented in IFCI. This approach is described in Section 4.1.9.

Finally, in Sections 4.1.10 through 4.1.12, a description will be given of the major assumptions and simplifications, how the models are actually coded, and the status of model assessment.

4.1.1 Coefficients, Velocities, and Diameters

Throughout this discussion of the two-phase interfacial heat transfer modeling in IFCI, a number of basic equations and definitions will be applied over and over. In this sub-section these parameters and definitions are defined and described, together with the correlations that are associated with them.

In IFCI, the total heat transfer from the vapor to the water, Q_{12}, is always assumed to be the sum of two contributions: vapor to an interface at the saturation temperature, T_{sat}, and this interface to the water. This can be expressed as

$$Q_{12} = h_{i1} A_{12} (T_1 - T_{sat}) + h_{i2} A_{12} (T_{sat} - T_2) \quad (4.1)$$

where

T_{sat} = the saturation temperature of steam evaluated at the partial pressure of the vapor,
A_{12} = the interfacial surface area between the vapor and water,
h_{i1} = the vapor-to-interface heat transfer coefficient, and
h_{i2} = the interface-to-water heat transfer coefficient.

Of great importance in calculating the interfacial heat transfer are a number of velocities associated with the different fields. These are described next.

Consider the control volume illustrated in Figure 4-1 and the water and vapor velocities shown. A cell centered velocity difference between the water and vapor fields is calculated as follows.

Given the velocities as shown in Figure 4-1, average cell centered water velocities are calculated and then used to find a vector water velocity, a vector vapor velocity, and a vector water-vapor velocity difference.

$$\overline{W}_2 = 0.5 (W_{2,j} + W_{2,j-1}) \quad (4.2a)$$

$$\overline{W}_1 = 0.5 (W_{1,j} + W_{1,j-1}) \quad (4.2b)$$

$$\overline{U}_2 = 0.5 (U_{2,i} + U_{2,i-1}) \quad (4.2c)$$

$$\overline{U}_1 = 0.5 (U_{1,i} + U_{1,i-1}) \quad (4.2d)$$

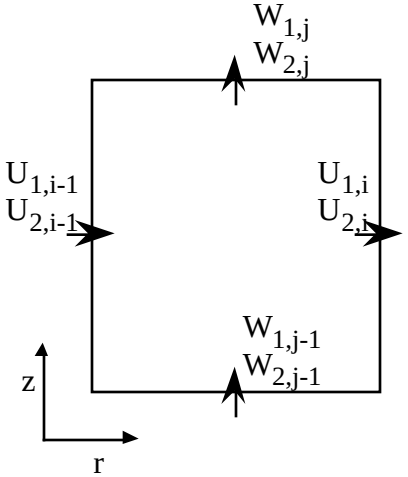

Figure 4-1 Water and Vapor Velocities Around a Typical Control Volume

$$V_L = \sqrt{\overline{W}_2^{\,2} + \overline{U}_2^{\,2}} \tag{4.3}$$

$$V_V = \sqrt{\overline{W}_1^{\,2} + \overline{U}_1^{\,2}} \tag{4.4}$$

$$V_{12} = \text{Max}\left(\sqrt{\left(\overline{W}_2 - \overline{W}_1\right)^2 + \left(\overline{U}_2 - \overline{U}_1\right)^2}\,,\, 10^{-3}\right) \tag{4.5}$$

We next turn our attention to the calculation of droplet and bubble diameters. These are generally found by use of a constant Weber number assumption (in IFCI (as in TRAC), a constant value of 7.5 is used for bubbles, and a value of 4.0 for droplets). However, in IFCI this approach has been modified by the addition of a number of constraints which are intended to limit the possible values by physically based bounds. To describe the total approach, it is useful to first list a number of equations and definitions.

First we note that by definition, the generic expression for the Weber number of a spherical bubble or droplet can be written as

$$We = \frac{\rho (V_{rel})^2 D}{\sigma}\,, \tag{4.6}$$

where

σ = surface tension of the liquid phase (water). Calculated as a function of pressure and saturation temperature (See Section 6).
ρ = the density of the fluid medium surrounding the droplet or bubble
D = the bubble or droplet diameter, and
V_{rel} = relative velocity between the vapor and water

Next we define a hydraulic diameter, D_h, also to be used later. In IFCI, the hydraulic diameter is defined in terms of a cell flow volume, fvol, and a wetted surface area, SA, instead of the normal flow cross section, A_{cross},and wetted perimeter, P_{wett}.

$$D_h = \frac{4*fvol}{SA} \approx \frac{4*A_{cross}}{P_{wett}} \tag{4.7}$$

We now turn our attention to calculating a bubble diameter and bubble Reynolds number to be used in the bubbly flow and slug flow regimes. The physical situation envisioned is a mass of vapor bubbles surrounded by liquid water. We begin by defining a maximum bubble diameter;

$$D_{b,max} = \text{Max}\left(\ \text{Min}\left\{D_{b,rise}\,,\, D_{b,mass}\right\}\,,\, D_{min}\right) \tag{4.8}$$

where

$$D_{b,rise} = \sqrt{\frac{0.75\ We\ \sigma\ \rho_1}{\rho_2\ g\ (\rho_2-\rho_1)}}, \quad We = 7.5 \tag{4.9}$$

$$D_{b,mass} = \left(\frac{6\,\alpha_1\,Vol}{\pi}\right)^{1/3} \tag{4.10}$$

$$D_{min} = .0001\ m \tag{4.11}$$

The diameter $D_{b,max}$ is used in finding a bubble rise velocity, V_{rise}, characterizing a bounding maximum velocity between bubbles and the surrounding water, if bubbles were rising under the force of buoyancy. Eq. (4.9) is derived by assuming a Weber number of 7.5, a drag coefficient between the bubble and water of 1.0, and balancing gravitational and drag forces. It is an upper bound because it does not account for viscous effects. Equation (4.10) is the diameter of a spherical bubble containing all of the vapor within the given control volume (Vol = volume of the control volume), another physically based upper bound on the size of the bubble. The value of D_{min} given in Eq. (4.11) is an arbitrary lower limit (contained in a data statement in the code) which is applied.

Once the value of $D_{b,max}$ is calculated from Eq. (4.8) a rise velocity, V_{rise}, is calculated by assuming a drag coefficient between the bubble and water of 1.0, and balancing gravitational and drag forces (see Eq. 8.5 in Reference [15]), yielding

$$V_{rise} = \sqrt{\frac{4}{3}\,D_{b,max}\,g\left(\frac{\rho_2-\rho_1}{\rho_1}\right)} \tag{4.12}$$

This velocity is used as an upper bound on the relative velocity between the vapor bubble and the water, V_{rb}, used in calculating the bubble diameter, D_b, and bubble Reynolds number, Re_b. Thus the following three equations are applied.

$$V_{rb} = Max\ (\ V_{rise}, V_{12}\ ) \tag{4.13}$$

$$D_b = Min\left(Max\left\{\frac{\sigma\ We_b}{\rho_2\ (V_{rb})^2}, D_{min}\right\}, D_h, D_{b,max}\right)\ ;\ We_b = 7.5 \tag{4.14}$$

$$Re_b = \frac{\rho_2\,|V_{rb}|\,D_b}{\mu_2}\ . \tag{4.15}$$

Another set of equations, completely analogous to Eqs. (4.8) through (4.15) is used to calculate a droplet diameter, D_d, and droplet Reynolds number, Re_d. In this case we envision droplets of liquid water surrounded by gaseous vapor. Thus the idea of a terminal velocity is substituted for that of the rise velocity used above. Also, an additional constraint reducing the droplet diameter in superheated conditions is applyed. These equations are given below in sequence, but without further explanation.

$$D_{b,max} = \text{Max}\left(\text{Min}\left\{ D_{b,rise} , D_{b,mass} \right\} , D_{min} \right) \tag{4.16}$$

where

$$D_{d,term} = \sqrt{\frac{0.75\ We\ \sigma\ \rho_2}{\rho_1\ g\ (\rho_2-\rho_1)}}, \quad We = 4.0 \tag{4.17}$$

$$D_{d,mass} = \left(\frac{6\,\alpha_2\,Vol}{\pi} \right)^{1/3} \tag{4.18}$$

$$D_{min} = .0001\ \text{m} \tag{4.19}$$

$$V_{term} = \sqrt{\frac{4}{3} D_{d,max}\ g \left(\frac{\rho_2-\rho_1}{\rho_2} \right)} \tag{4.20}$$

$$V_{rd} = \text{Max}\ (\ V_{term}, V_{12}\ ) \tag{4.21}$$

$$D_d' = \frac{\sigma\ We_d}{\rho_1\ (V_{rd})^2} \quad ; \quad We_d = 4.0 \tag{4.22}$$

To adjust for superheated conditions, IFCI does the following:

We let $$F1 = \text{Max}\left(0.0 , \text{Min}\left\{ \frac{(T_1 - T_{sat}) - 2.0}{20} , 1.0 \right\} \right) \tag{4.23}$$

then find $$D_d'' = F1 * D_{min} + (1-F1)*D_d' \tag{4.24}$$

The droplet diameter and droplet Reynolds number are now calculated as

$$D_d = \text{Min}\left(\text{Max}\left\{ D_d'' , D_{min} \right\}, D_h, D_{d,mass} \right) \; ; \; We_d = 4.0 \tag{4.25}$$

$$Re_d = \frac{\rho_2 |V_{rd}| D_d}{\mu_2} \; . \tag{4.26}$$

Finally, given the values of the relative bubble velocity, V_{rb}, and the relative droplet velocity, V_{rd}, from Equations (4.13) and (4.21), the vector relative velocity, V_{12}, is bounded by these values.

$$V_{12} = \text{Max}\left(V_{rb}, V_{rd} , V_{12} \right) \tag{4.27}$$

4.1.2 Vertical Bubbly Flow Regime

For $\alpha_v' < 0.3$, correlations developed for the bubbly flow regime are used to determine the interfacial heat transfer.

4.1.2.1 Interfacial Surface Area

In vertical bubbly flow, the interfacial surface area A_{12} is calculated in conjunction with a critical bubble Weber number as explained above in Section 4.1.1. Given the value of D_b (see Eq. (4.14)), and with the assumption of a uniform bubble distribution within the control volume, the number of bubbles is

$$CNB = \frac{6 \alpha_1 Vol}{\pi D_b^3} \; , \tag{4.28}$$

where "Vol" is the volume of the control volume, and α_1 is the vapor volume fraction.

Assuming the bubble surface area can be found from the surface area of a sphere, the interfacial area can be found as

$$A_{12} = 6 \alpha_1 \left(\frac{Vol}{D_b} \right) \tag{4.29}$$

In TRAC, this value is restricted from becoming smaller than a value based on a minimum number density of bubbles. This restriction was removed from the IFCI formulation when situations arose which appeared to produce physically unreasonable results.

4.1.2.2 Vapor-to-Interface Heat Transfer Coefficient

In the bubbly regime, the vapor-to-interface heat transfer coefficient, h_{i1}, is set equal to a constant.

$$h_{i1} = 1000. \tag{4.30}$$

This is a simplification of the TRAC formulation which uses a different constant (h_{i1} = 10,000) if the vapor temperature is in the nonequilibrium condition $T_1 > T_{sat}$.

4.1.2.3 Interface-to-Water Heat Transfer Coefficient

The interface-to-water heat transfer coefficient is found from the larger of two correlations: the approximate formulation of the Plesset-Zwick bubble growth model [16,17], and a modification of a convective heat transfer correlation suggested by Lee and Ryley [18]. Expressed in terms of a Nusselt number, this can be written as

$$Nu_{i2} = \frac{h_{i2} D_b}{k_2} = \text{Max}\left(Nu_{PZ}, Nu_{LR}\right) \tag{4.31}$$

The correlations for the two Nusselt numbers are

$$Nu_{PZ} = \frac{12}{\pi} (T_{sat} - T_2) \frac{\rho_2}{\rho_1 L} \frac{\partial u_2}{\partial T_2} \tag{4.32}$$

and

$$Nu_{LR} = 2.0 + 0.74\, Re_b^{0.5} \tag{4.33}$$

where

L = latent heat of vaporization
u_2 = the internal energy of the water

We note that this is a simplification of the TRAC formulation which uses a different correlation (Stanton Number = .02) if the water temperature is in the nonequilibrium condition $T_2 < T_{sat}$.

4.1.3 Vertical Slug Flow Regime

The slug flow regime is considered to exist in vertical flow when the normalized vapor volume fraction, α_v', is in the range from 0.3 to 0.5. We note that in this regime, IFCI has adopted a formulation which has some differences with the formulation used in the TRAC code. The

conceptual picture is that as the volume fraction increases, the individual bubbles begin to agglomerate and form plugs or slugs of vapor. At a maximum α_v' of 0.5, 40% of the vapor is assumed to exist in the form of trailing bubbles, with the remainder contained in slugs whose diameter is equal to the hydraulic diameter of the flow channel. In this regime the interfacial heat transfer coefficients are calculated as a weighted sum between that portion which is still considered to be bubbly-like flow, and that portion considered as a pure slug flow. The application of the IFCI approach can best be illustrated by considering the following steps:

Step 1: In addition to a bubble diameter, D_b, found by using Eq. (4.14), calculate an effective diameter of the slug, D_s, by interpolation on α_v'.

$$D_s = (1-f_1) * D_b + f_1 * D_h \tag{4.34}$$

where the interpolating function f_1 is defined as

$$f_1 = \frac{(\alpha_v' - 0.3)}{0.2} \quad , \qquad 0.3 < \alpha_v' < 0.5 \quad , \tag{4.35}$$

and where

D_h = hydraulic diameter (see Eq. (4.7))

Using the interpolating function f_1 again, calculate the separate volume fractions associated with that portion of the vapor assumed to be in bubbles and that portion which is assumed to be in the form of slugs.

$$\alpha_b = \alpha_1 [\, 1 - (0.6 * f_1)] \tag{4.36}$$

$$\alpha_s = \alpha_1 (0.6 * f_1) \tag{4.37}$$

Step 2: Calculate both the vapor-to-interface heat transfer coefficient, h_{i1}, and the interface-to-water heat transfer coefficient, h_{i2}, as follows

$$h_{i1} = 1000 \quad , \text{ and} \tag{4.38}$$

$$h_{i2} = \left(2.0 + 0.74 \, Re_b^{0.5} \right) \frac{k_2}{D_b} \quad , \tag{4.39}$$

where Eq. (4.39) uses the convective heat transfer correlation suggested by Lee and Ryley [18], and h_{i1} in Eq. (4.38) is the same constant value as given in (4.30).

Step 3: Calculate the interfacial surface area, A_{12}, as a weighted sum between that portion which is still considered to be bubbly-like flow, and that portion considered as a pure slug flow. To do this use a modified form of Eq. (4.29) derived earlier.

$$A_{12} = 6\,\mathrm{Vol}\left(\frac{\alpha_b}{D_b} + \frac{\alpha_s}{D_s}\right) \tag{4.40}$$

This method is an add hoc approach, but does provide for a continuous representation of the behavior of the interfacial heat transfer as the vapor volume fraction crosses the value of 0.3 (marking the boundary between bubbly and slug flow) and increases toward 0.5.

4.1.4 Vertical Mist Flow Regime

The vertical mist flow regime is considered to exist in vertical flow when the normalized vapor volume fraction, α_v', is greater than 0.75. In IFCI, the interface-to-water heat transfer coefficient, h_{i2}, is calculated using the convective heat transfer correlation suggested by Lee and Ryley [18], but is constrained by a maximum value of 50000. The vapor-to-interface heat transfer coefficient, h_{i1}, is calculated by assuming a constant Stanton number of .02, but is constrained to a minimum value of 1000.

$$h_{i2} = \mathrm{Min}\left(50000,\ 0.02\,\rho_2\,Cp_2\,|V_r|\right) \tag{4.41}$$

$$h_{i1} = \mathrm{Max}\left(1000,\ \left(2.0 + 0.74\,Re_d^{0.5}\right)\frac{k_1}{D_d}\right) \tag{4.42}$$

$$A_{12} = 6\,\alpha_2\left(\frac{\mathrm{Vol}}{D_d}\right) \tag{4.43}$$

In determining the droplet diameter, D_d, we note that a constant droplet Weber number of We_d = 4.0 is assumed. According to Reference [5] (see pg. 6-27), sensitivity tests on the effect of droplet Weber number have shown that variations between 2 and 12 did not strongly influence the results, although Hinze [19] recommended a value of 3.46. In IFCI we adopt the TRAC value of 4.0.

4.1.5 Vertical Transition Flow Regime

The interpolated or transition flow regime is considered to exist in vertical flow when the normalized vapor volume fraction, α_v', is in the range from 0.5 to 0.75. In this regime, the interfacial heat transfer coefficients and surface areas are found by linearly interpolating

between the values which would be calculated at the top edge of the slug flow regime ($\alpha_v' = 0.5$) and the bottom edge of the annular mist regime ($\alpha_v' = 0.75$).

The application of this approach can be illustrated as follows:

Step 1: Calculate two sets of values for the interfacial heat transfer coefficients and surface areas, one set corresponding to slug flow when $\alpha_v' = 0.5$, the other corresponding to mist flow when $\alpha_v' = 0.75$. Applying equations (4.38) through (4.43) we can write

$$h_{i1,slug} = 1000 \text{ , and} \tag{4.44}$$

$$h_{i2,slug} = \left(2.0 + 0.74\, Re_b^{0.5} \right) \frac{k_2}{D_b} \text{ ,} \tag{4.45}$$

$$A_{12,slug} = 6\, Vol \left(\frac{.4\,\alpha_1}{D_b} + \frac{.6\,\alpha_1}{D_h} \right) \tag{4.46}$$

and

$$h_{i2,mist} = Min \left(50000,\ 0.02\, \rho_2\ Cp_2\ |V_{12}| \right) \tag{4.47}$$

$$h_{i1,mist} = \left(2.0 + 0.74\, Re_d^{0.5} \right) \frac{k_1}{D_d} \tag{4.48}$$

$$A_{12,mist} = 6 * .25 \left(\frac{Vol}{D_d} \right) \tag{4.49}$$

Step 2: Interpolate between the set of values as follows:

$$h_{i1} = (1\text{-}f_1) * h_{i1,slug} + f_1 * h_{i1,mist} \tag{4.50}$$

$$h_{i2} = (1\text{-}f_1) * h_{i2,slug} + f_1 * h_{i2,mist} \tag{4.51}$$

$$A_{12} = (1\text{-}f_1) * A_{12,slug} + f_1 * A_{12,mist} \tag{4.52}$$

where the interpolating function f_1 is defined here as

$$f_1 = \frac{(\alpha_v' - 0.5)}{0.25}, \quad 0.5 < \alpha_v' < 0.75 \text{ .} \tag{4.53}$$

We note that the difference between the interpolation method employed by IFCI and that used in the current version of TRAC is that TRAC uses a cubic interpolating function instead of a linear function.

4.1.6 Horizontal Stratified Flow Regime

The horizontal stratified flow regime is assumed to exist when the corrected water flux, G'_L, is below 2000 kg/(m^{2}s) and the corrected vapor flux, G'_V, is less then 4.0 kg/(m^{2}s). In this regime the convective heat transfer correlation suggested by Lee and Ryley [18] is used for both the interface-to-water heat transfer coefficient and the vapor-to-interface heat transfer coefficient. Note that in order to indicate horizontal flow conditions, an additional subscript h has been added to the characters.

$$h_{i2h} = \text{Max}\left(5000, \left(2.0 + 0.74\, Re_2^{0.5} \right) \frac{k_2}{D_h} \right) \tag{4.54}$$

$$h_{i1h} = \left(2.0 + 0.74\, Re_1^{0.5} \right) \frac{k_1}{D_h} \tag{4.55}$$

where the water and vapor Reynolds numbers are based on the hydraulic diameter as follows:

$$Re_2 = \frac{\rho_2 V_L D_h}{\mu_2} \tag{4.56}$$

$$Re_1 = \frac{\rho_1 V_V D_h}{\mu_1} \quad . \tag{4.57}$$

Note that the water and vapor velocities used in these Reynolds numbers were previously defined in Eqs. (4.3) and (4.4). Also, since the flow is considered stratified, the interfacial area, A_{12}, is set equal to the axial flow area.

4.1.7 Horizontal Mist Flow Regime

The mist (or annular mist) flow regime is considered to exist in horizontal flow when the corrected water flux, G'_L, is below 2000 kg/(m^{2}s) and the corrected vapor flux, G'_V, is greater than 4.0 kg/(m^{2}s). However, to avoid the possibility of a sharp discontinuity in calculated values, an interpolation is made in the range $4 < G'_V < 30$. The calculation begins by finding the interfacial heat transfer coefficients and interfacial area in the same manner as was previously described for vertical mist flow.

$$h_{i2,mist} = \text{Min}\left(50000,\ 0.02\, \rho_2\ Cp_2\ |V_r| \right) \tag{4.58}$$

$$h_{i1,mist} = \text{Max}\left(1000,\ \left(2.0 + 0.74\, Re_d^{0.5} \right) \frac{k_1}{D_d} \right) \tag{4.59}$$

$$A_{12,mist} = 6\,\alpha_2\left(\frac{Vol}{D_d}\right) \tag{4.60}$$

Next, if the value of the corrected vapor flux is such that $4 < G_V' < 30$, then the values are adjusted based on the following. Let

$$F1 = Min\left(1.0\,,\frac{(G_L' - 4)}{26}\right)\quad, \tag{4.61}$$

then

$$h_{i1h} = (1\text{-}F1)\,h_{i1h,strat} + F1\,h_{i1h,mist} \tag{4.62}$$

$$h_{i2h} = (1\text{-}F1)\,h_{i2h,strat} + F1\,h_{i2h,mist} \tag{4.63}$$

$$A_{i1h} = (1\text{-}F1)\,A_{i1h,strat} + F1\,A_{i1h,mist} \tag{4.64}$$

where in these equations the subscript "strat" indicates values that were calculated for stratified flow (Eqs. (4.54) through (4.55)).

4.1.8 Horizontal Bubbly Flow Regime

The horizontal bubbly flow regime is considered to exist when the corrected water flux, G_L', is greater than 2000 kg/(m^{2}s). However, to avoid the possibility of a sharp discontinuity in calculated values, an interpolation is made in the range $2000 < G_L' < 5000$. The calculation begins by finding the interfacial heat transfer coefficients and interfacial area in the same manner as was previously described for vertical bubbly flow.

$$h_{i1h,bub} = 1000. \tag{4.65}$$

$$h_{i2h,bub} = \left(2.0 + 0.74\,Re_b^{0.5}\right)\frac{k_2}{D_b}\quad, \tag{4.66}$$

$$A_{12h,bub} = 6\,\alpha_1\left(\frac{Vol}{D_b}\right) \tag{4.67}$$

Next, if the value of the corrected water flux is such that $2000 < G_L' < 5000$, then the values are adjusted based on the following. Let

$$F1 = Min\left(1.0\,,\frac{(G_L' - 2000)}{3000}\right)\quad, \tag{4.68}$$

then

$$h_{i1h} = (1\text{-}F1)\,h_{i1h,other} + F1\,h_{i1h,bub} \tag{4.69}$$

$$h_{i2h} = (1\text{-}F1)\,h_{i2h,other} + F1\,h_{i2h,bub} \tag{4.70}$$

$$A_{i1h} = (1\text{-}F1)\,A_{i1h,other} + F1\,A_{i1h,bub} \tag{4.71}$$

where in these equations the subscript "other" indicates values that were calculated for either stratified flow (Eqs. (4.54) through (4.55)) or mist flow (Eqs. (4.62) through (4.64)).

4.1.9 Interpolation Between Horizontal and Vertical Regimes

When a difference exists between the flow regime calculated from the horizontal flow map and the vertical flow map, an interpolation scheme is applied. To find the interpolated heat transfer coefficients, IFCI uses

$$h_{i1} = (1\text{-FZR})\, h_{i1v} + \text{FZR}\, h_{i1h} \tag{4.72}$$

$$h_{i2} = (1\text{-FZR})\, h_{i2v} + \text{FZR}\, h_{i2h} \tag{4.73}$$

where the additional subscripts "v" and "h" refer to values calculated from the vertical flow regime correlations (Sections 4.1.2 through 4.1.5) and the horizontal flow regime correlations (Sections 4.1.6 through 4.1.8) respectively. The interpolating function FZR is found as a function of calculated mass flux ratios.

$$\text{FZR} = \frac{\text{GMR}}{\text{GMA}} \tag{4.74}$$

where

$$\text{GMA} = \alpha_v'\ \rho_1\, V_V + (1 - \alpha_v')\, \rho_2\, V_L \tag{4.75}$$

$$\text{GMR} = \alpha_v'\ \rho_1\, \overline{U}_1 + (1 - \alpha_v')\, \rho_2\, \overline{U}_2 \tag{4.76}$$

If the horizontal flow map indicates stratified flow, then the interfacial area must also be interpolated. This is done by adding the value of the stratified-flow interfacial area, A_{i1h}, to a portion of the interfacial area calculated from the vertical flow regime map, A_{i1v}.

$$A_{i1} = \frac{\text{GVZ}}{\text{GV}} A_{i1v} + A_{i1h} \tag{4.77}$$

where

$$\text{GVZ} = \text{Max}\left(\text{AL10}\ \rho_1\, V_{rise}\, ,\, \alpha_1\ \rho_1\, |\overline{W}_1| \right) \tag{4.78}$$

$$\text{GVR} = \alpha_1\ \rho_1\, |\overline{U}_1| \tag{4.79}$$

$$\text{GV} = \sqrt{\text{GVR}^2 + \text{GVZ}^2} \tag{4.80}$$

and where the value of AL10 (see Eq. 4.78), is a user specified input - a small number usually on the order of 10^{-5}.

4.1.10 Review of Major Assumptions

The models used in calculating the interfacial heat transfer coefficients and interfacial areas contain many fundamental assumptions. The major assumptions used are as follows:

1. It is assumed that the bubble and droplet diameters can be determined using a constant Weber-number criterion. For bubbles it is assumed that $We_b = 7.5$, for droplets that $We_d = 4.0$. Such a model assumes an equilibrium between inertia and surface tension forces.
2. The transients are assumed to be slow enough that the flow regimes and the heat transfer coefficients can be determined using the quasi-steady approach.
3. Bubbles or droplets are assumed to be uniformly distributed within the control volume.
4. Surface areas of bubbles and droplets can be found by assuming spherical geometry.
5. It is assumed that two dimensional flow conditions can be adequately accounted for by an interpolation between one dimensional vertical and horizontal flow regime maps as explained in Section 4.1.9

In addition to these five assumptions, each flow regime has assumed that certain correlations or constants are valid approximations for calculating the interfacial heat transfer coefficients over the entire flow regime.

4.1.11 Comments on Assessment

Many of the models used in calculating the interfacial heat transfer coefficients and interfacial areas were adopted directly from the TRAC code. Reference [5] reviews the TRAC models and provides some assessment of the modeling. However, even this is incomplete and further assessment was recommended. The additional modeling which has been included in IFCI, although following the spirit of the TRAC approach, has not yet been directly assessed.

4.2 Heat Transfer Between Melt (Field 3) and Fields 1 and 2 (Vapor and Water)

In IFCI, melt is assumed for heat transfer purposes to have the geometric character of a collection of simple spherical particles, each of given diameter D_c, and dispersed uniformly throughout the available flow volume. Of interest in this section is the heat transfer between the melt particles and a surrounding water-vapor fluid.

When condensation is not being modeled, the heat transfer rate between the melt and field j (j=1 or 2) is given by

$$q_{3j} = a_{3j}\, h_{3j}\, (T_3 - T_j) \tag{4.82a}$$

where a_{3j} is the interfacial surface area between the melt and field j per unit volume, and is calculated as follows.

$$a_{3j} = \frac{6\,\alpha_3}{D_c} \tag{4.82b}$$

The focus of this section will be the determination of the heat transfer coefficients h_{3j}.

Three different heat transfer regions are described in Table 3.5. Both forced and natural convection are considered in Region I (However, it should be noted that not all this domain can be realized during reactor accidents.) In region II, nucleate, transition, and film boiling heat transfer regimes are modeled. Region III is a region where interpolation is applied so that the heat transfer values behave smoothly as the flow conditions change from pure convection to boiling.

In the correlations that are applied, the important velocities will be relative velocities between the different fields. In particular, the velocity difference between the melt and water, and between the melt and vapor are important. These values are defined in IFCI in the same way the the relative velocities between fields one and two are (see Eqs. (4.2) through (4.5) and Figure 3-5).

$$\overline{W}_3 = 0.5\,(\,W_{3,j} + W_{3,j-1}) \tag{4.83}$$

$$\overline{U}_3 = 0.5\,(U_{3,i} + U_{3,i-1}) \tag{4.84}$$

$$V_C = \sqrt{\overline{W}_3^{\,2} + \overline{U}_3^{\,2}} \tag{4.85}$$

$$V_{13} = \mathrm{Max}\left(\sqrt{\left(\overline{W}_3 - \overline{W}_1\right)^2 + \left(\overline{U}_3 - \overline{U}_1\right)^2}\,,\, 10^{-3}\right) \tag{4.86}$$

$$V_{23} = \text{Max}\left(\sqrt{\left(\overline{W}_3 - \overline{W}_2\right)^2 + \left(\overline{U}_3 - \overline{U}_2\right)^2}\,,\, 10^{-3}\right) \tag{4.87}$$

Table 3.5 Interfacial Heat Transfer Regions for Melt in the Presence of Fields 1 and/or 2

Region	Conditions
I. Pure Convection	$\alpha_v' > 0.98$
	$T_3 \le T_{sat}$, or $T_3 \le T_2$
	$P \ge P_{crit}$
II. Pure Boiling	$\alpha_v' < 0.5$
	$T_3 \ge T_{sat} + 5$
	$T_3 > T_2$
	$P < P_{crit}$
III. Interpolation	$0.5 \le \alpha_v' \le 0.98$
	$T_{sat} < T_3 < T_{sat} + 5$
	$T_3 > T_2$
	$P < P_{crit}$

4.2.1 Pure Convection

The melt-vapor and melt-water heat transfer coefficients are calculated as an appropriate single phase value weighted by a simple (add-hoc) function of the normalized vapor volume fraction.

$$h_{31} = (1 - \mathbf{f}(\alpha_v'))\, h_1 \tag{4.88}$$

$$h_{32} = \mathbf{f}(\alpha_v')\, h_2 \tag{4.89}$$

where

$$\mathbf{f}(\alpha_v') = \max\left\{0.,\ \min\left[1.,\ \frac{(0.75-\alpha_v')}{0.5}\right]\right\}$$

Note that the function $\mathbf{f}(\alpha_v')$ requires that the convective melt-vapor heat transfer be zero for α_v' below 0.25, and the convective melt-water heat transfer to be zero for α_v' greater than 0.75.

Both single phase heat transfer coefficients (h_{31} and h_{32}) are calculated using the same correlations, and both natural and forced convection regimes are considered. Using the

subscript "f" to denote either the field 1 or field two coefficient, the correlations currently used in IFCI (Reference [20], pgs 409, 413) are as follows.

$$Nu_f = \frac{h_f D_h}{k_f} = \begin{cases} Nu_{nc} & \mathbf{r} = Gr/(Re)^2 > 1 \\ \mathbf{r}\, Nu_{nc} + (1-\mathbf{r})\, Nu_{fc} & \mathbf{r} = Gr/(Re)^2 < 1 \end{cases} \quad (4.90)$$

where

$$Nu_{nc} = 2.0 + 0.6\, Gr_f^{1/4}\, Pr_f^{1/3} \quad (4.91)$$

$$Nu_{fc} = 2.0 + 0.6\, Re_f^{1/2}\, Pr_f^{1/3} \quad (4.92)$$

and where the Reynolds number, Grashof number, and Prandtl number are defined as

$$Re_f = \frac{\alpha_f \rho_f V_{f3} D_h}{\mu_f} \quad , \quad (4.93)$$

$$Gr_f = \frac{\alpha_f^2 g \beta_f (D_h)^3 (T_3 - T_f)}{\nu_f^2} \quad , \text{ and} \quad (4.94)$$

$$Pr_f = \frac{\mu_f C_{pf}}{k_f} \quad . \quad (4.95)$$

Note that the ratio, $r = Gr/(Re)^2$, determines the importance of natural convection in each case.

4.2.1 Pure Boiling

Heat transfer coefficients that account for boiling are calculated whenever the melt temperature, T_3, is greater than T_{sat}, and the modified vapor fraction, α_v', is less than 0.98. However, as will be described in detail in Section 4.2.3, interpolation is used when $T_{sat} < T_3 < (T_{sat} + 5)$ and when $0.75 \le \alpha_v' \le 0.98$. When $T_3 \ge T_{sat} + 5$ and $\alpha_v' < 0.75$, the correlations discussed in this section are used without modifications.

Depending on the temperature of the melt, either nucleate, transition, or film boiling is considered to be occurring. Nucleate boiling occurs when the melt temperature is greater than T_{sat} but less than T_{CHF}, the temperature corresponding to the critical heat flux. Film boiling is modeled when the melt temperature is greater than T_{min}, the minimum film boiling temperature. Transition boiling is modeled in the intermediate range, $T_{CHF} < T_3 < T_{min}$. In each of these regimes, a heat transfer coefficient between the melt and both the liquid water, h_{32}, and gaseous vapor, h_{31}, must be calculated.

4.2.2.1 Nucleate Boiling

The modeling in IFCI for Nucleate boiling between melt and a two-phase steam water mixture is modeled in much the same way as described in Reference [4] for the TRAC code as it existed in 1986. Although some modifications to this approach were subsequently been made in TRAC, the material presented in Reference [5] is also largely still applicable to IFCI. The discussion presented here is adopted from References [4] and [5] will only review the basis of this model as applied in the HTMELT subroutine.

Melt to Water heat transfer coefficient, h_{32}

The Chen correlation (see [21], p. 262) is used in the nucleate boiling heat-transfer regime. The Chen correlation assumes that both nucleation and convective mechanisms occur and that the contributions made by the two mechanisms are additive.

$$h_{32} = h_{fc} + \min\left[1, \frac{(T_3 - T_{sat})}{(T_3 - T_2)}\right] h_{nb} \tag{4.96}$$

The forced convective component, h_{fc}, is assumed to be represented by the maximum of a Dittus-Boelter type of turbulent flow equation (modified by the so called F factor) and the Rohsenow-Choi laminar flow equation:

$$h_{fc} = \max[h_{tfc}, h_{lfc}] \tag{4.97}$$

where

$$h_{lfc} = 4.0 \frac{k_2}{D_c}, \tag{4.98}$$

and

$$h_{tfc} = 0.023 \frac{k_2}{D_c} \left[\frac{\rho_2 V_{23}(1-\alpha_v')D_c}{\mu_2}\right]^{0.8} Pr_2^{0.4} * F. \tag{4.99}$$

The parameter, F > 1.0, is used to modify the convective part of the correlation (called the macroterm), to account for increased agitation caused by the formation of vapor bubbles. The "F" factor is found as a function of the Martinelli factor, X_{TT}^{-1}:

$$F = \begin{cases} 1.0 & , \; X_{TT}^{-1} \le 0.10 \\ 2.35\left(X_{TT}^{-1} + 0.213\right)^{0.736} & , \; X_{TT}^{-1} > 0.10 \end{cases} \tag{4.100}$$

with

$$X_{TT}^{-1} = \left(\text{Martinelli factor}\right)^{-1} = \left(\frac{x}{1-x}\right)^{0.9} \left(\frac{\rho_2}{\rho_1}\right)^{0.5} \left(\frac{\mu_2}{\mu_1}\right)^{0.1} \; , \tag{4.101}$$

and where X_{TT}^{-1} is limited to a maximum value of 100.

The basis for the nucleate boiling component, h_{nb}, is the analysis of Forster and Zuber [22] for pool boiling. This has been modified by a suppression factor, S, to account for the difference between the wall superheat and the mean superheat to which the bubble is exposed.

$$h_{nb} = S * 0.00122 \left(\frac{k_2^{0.79} \, Cp_2^{0.45} \, \rho_2^{0.49}}{\sigma^{0.5} \mu_2^{0.29} \, L^{0.24} \, \rho_1^{0.24}}\right) (T_3 - T_s)^{0.24} \; (P_w - P)^{0.75} \tag{4.102}$$

For values of $\alpha_v' < 0.7$, the S factor is calculated as

$$S = \begin{cases} \left[1.0 + 0.12\left(Re_{tp}\right)^{1.14}\right]^{-1}, & 0.0 < Re_{tp} < 32.5 \\ \left[1.0 + 0.42\left(Re_{tp}\right)^{0.78}\right]^{-1} & , \; 32.5 \le Re_{tp} \le 70.0 \end{cases} \tag{4.103}$$

where

$$Re_{tp} = \min\left[\left(\frac{\rho_2 V_{23} (1 - \alpha_v') D_C}{\mu_2} \right) F^{1.25} \; , \; 70.0 \right] \tag{4.104}$$

Because Eqs. (4.103) do not approach the correct limit of zero as α_v' goes to 1, an additional modification is imposed for values of α_v' greater than 0.7. To ensure that S approaches the correct value for $\alpha = 1.0$, the following procedure is used. When $\alpha > 0.70$, S is evaluated at $\alpha = 0.70$ and the current value of α; the minimum of the two values, S_{min}, is saved. Linear interpolation is then used between the two values, S_{min} and S = 0.0 at $\alpha_c = 0.98$. That is,

$$S = \begin{cases} S_{min}\,\dfrac{(0.98 - \alpha)}{(0.98 - 0.70)}\ , & \alpha > 0.70 \\ 0.0\ , & \alpha > 0.98 \end{cases} \qquad (4.105)$$

Melt to Vapor heat transfer coefficient, h_{31}

The melt-to-vapor convective heat transfer coefficient is calculated to go from zero at $T_3 = T_s$, to the transition boiling value at $T_3 = T_{CHF}$. It is defined as follows:

Let

$$y = \frac{(T_3 - T_s)}{(T_{CHF} - T_s)}\ , \qquad (4.106a)$$

then

$$h_{31} = (3y^2 - 2y^3) * h_{31,\,film\,(T_{CHF})}\ , \qquad (4.106b)$$

where "$h_{31,\,film\,(T_{CHF})}$" is found from the film boiling correlations described in 4.2.2.3 when $T_3 = T_{CHF}$.

4.2.2.2 Transition Boiling

The transition boiling regime spans the boiling surface between the critical heat flux (CHF) and minimum film boiling. In this model it is assumed that transition boiling heat transfer is composed of both nucleate-boiling (wet-wall) and film-boiling (dry-wall) heat transfer. This is based on the understanding that at a given location, the surface is wet part of the time and dry during the remainder of the time. Therefore, contributions to both the water and vapor heat transfer coefficients should exist for all conditions.

Melt to Water heat transfer coefficient, h_{32}

In IFCI, it is assumed that the heat transfer to the liquid water from the melt can be approximated as an interpolation between the critical heat flux (q_{CHF}) and the minimum stable film boiling heat flux (q_{min}). The value for the film boiling heat flux is, however, modified to account for radiation heat transfer (denoted $q_{min,rad}$). The interpolation equation applied is

$$q_{3\text{-}liq} = f_1\, q_{CHF} + (1\text{-}f_1) q_{min,rad} = h_{32}\,(T_3 - T_2)\,, \tag{4.107}$$

where

$$f_1 = (3y^2 - 2y^3)\,, \tag{4.108a}$$

$$y = \frac{(T_3 - T_{min})}{(T_{CHF} - T_{min})}\,. \tag{4.108b}$$

$$q_{min,rad} = q_{min} + \left[\sigma\,\varepsilon\,\frac{(T_3^4 - T_2^4)}{(T_3 - T_2)}\right](T_{min} - T_2) \tag{4.108c}$$

Given values for T_3, T_{min}, q_{min}, T_{CHF}, and q_{CHF}, and applying Eqs. (4.108), the value for h_{32} can be calculated directly by rearranging Eq. (4.107) as:

$$h_{32} = \frac{f_1\, q_{CHF} + (1\text{-}f_1) q_{min,rad}}{(T_3 - T_2)} \tag{4.109}$$

The method for calculating the values of T_{CHF} and q_{CHF} are described separately in Section 4.2.3.4. Likewise, the method for calculating the values of T_{min} and q_{min} is described in Section 4.2.3.5.

Vapor convective heat transfer coefficient, h_{31}

In IFCI, it is assumed that the heat transfer coefficient to the vapor can be approximated by interpolating between the value obtained at the critical heat flux ($h_{31,CHF}$) and the value obtained at the minimum stable film boiling heat flux ($h_{31,min}$). The interpolation equation applied is

$$h_{31} = f_1\, h_{31,CHF} + (1\text{-}f_1) h_{31,min}\,, \tag{4.110}$$

where the interpolating function f_1 is identical to the one given in Eq. (4.108);

$$f_1 = (3y^2 - 2y^3)\,, \tag{4.111a}$$

$$y = \frac{(T_3 - T_{min})}{(T_{CHF} - T_{min})}\,. \tag{4.111b}$$

The methods for calculating the values of T_{CHF} and q_{CHF} are described separately in Section 3.2.3.4. Likewise, the methods for calculating the values of T_{min} and q_{min} are described in Section 3.2.3.5.

4.2.2.3 Film Boiling

Melt to Water heat transfer coefficient, h_{32}

The film boiling heat transfer coefficient from the melt to the liquid water is given as

$$h_{32} = \text{Max}\left(h_{free}, h_{force} \right) + h_{rad} \tag{4.112}$$

where h_{free} and h_{force} are subcooled boiling correlations from Dhir and Purohit [23],

$$h_{free} = h_{sat} + h_{nat}\frac{(T_{sat} - T_2)}{(T_3 - T_{sat})} \tag{4.113}$$

where h_{sat} is given by the Bromley correlation [24],

$$h_{sat} = 0.8\left(\frac{\rho_1(\rho_2-\rho_1)\, g\, k_1^3\, h_{12}}{\mu_1\, D_c\, (T_3 - T_{sat})}\right)^{0.25} \tag{4.114}$$

(h_{12} is the latent heat of water) and h_{nat} is a natural convection correlation,

$$h_{nat} = 0.9\left(\frac{\rho_1^2\, g\, Cp_2\, (T_{sat} - T_2) k_1^3}{\mu_2\, D_c}\right)^{0.25} \tag{4.115}$$

The heat transfer coefficient h_{force} is a combination of the Bromley saturated boiling heat transfer coefficient h_{sat} (above) and a forced convection heat transfer correlation,

$$h_{force} = h_{sat} + 0.8\sqrt{Re}\left(1 + \frac{k_2\, (T_{sat} - T_2)}{k_1\, (T_3 - T_{sat})}\right)\frac{k_2}{D_c} \tag{4.116}$$

where

$$Re = \frac{(1-\alpha_v')\, \rho_2\, V_{23}\, D_c}{\mu_2} \tag{4.117}$$

The heat transfer coefficient from the film interface to the bulk liquid water is given by the greater of a natural convection correlation or a forced convection correlation [20]

$$h_{2s}^{c} = \text{Max}\left(Nu_{nc}, Nu_{fc}\right) \frac{k_2}{D_c} \tag{4.118}$$

where

$$Nu_{nc} = 2.0 + 0.6\, Gr_2^{1/4}\, Pr_2^{1/3} \tag{4.119}$$

$$Nu_{fc} = 2.0 + 0.6\, Re_2^{1/4}\, Pr_2^{1/3} \tag{4.120}$$

and where the Reynolds number, Grashof number, and Prandtl number are defined as

$$Re_2 = \frac{\rho_2 V_{23} D_c}{\mu_2} \quad , \tag{4.121}$$

$$Gr_2 = \frac{g\beta_2 (D_c)^3 (T_3 - T_2)}{\nu_2^2} \quad , \text{ and} \tag{4.122}$$

$$Pr_2 = \frac{\mu_2 C_{p2}}{k_2} \quad . \tag{4.123}$$

The radiation component of the melt to water heat transfer coefficient is found as

$$h_{rad} = \sigma \varepsilon \frac{(T_3^4 - T_2^4)}{(T_3 - T_2)} \tag{4.124}$$

Melt to Vapor heat transfer coefficient, h_{31}

In film boiling, melt to vapor heat transfer coefficient is currently set to zero. Note, however, that since the overall value of h_{31} is a sum of a boiling part and a convection part, its total value may not be zero.

4.2.3.4 Critical Heat Flux

If one considers a typical boiling curve, as the temperature of the surface increases to a point higher and higher above the fluid saturation temperature, a point is reached where the effective

heat transfer coefficient begins to deteriorate due to vapor blanketing. This point on the curve can be characterized by either the surface temperature, T_{CHF}, or the heat flux, q_{CHF}, at that point. The Critical Heat Flux (CHF) point has two purposes in relation to the IFCI boiling curve. First, the CHF point indicates the change from nucleate boiling regime to the transition boiling regime. Second, the CHF point is used in the quadratic interpolation that gives the transition-boiling liquid water heat transfer coefficient.

4.2.3.4.1 Basis of the Model

The critical heat flux prediction model used in IFCI was adopted directly from the TRAC code. The package consists of the Biasi correlation [25] with modifications at low mass velocities and high void fractions.

The Biasi correlation consists of taking the maximum of two equations; where one is typically appropriate for low quality, and the other for high quality. As applied in IFCI it can be expressed as follows:

$$q_{CHF} = 1.0 \times 10^4 \max \left[q_{CHF,lq}, q_{CHF,hq} \right] \tag{4.125a}$$

where

$$q_{CHF,lq} = \frac{1.883 \times 10^3}{(D_h)^n |G|^{1/6}} \left(\frac{f_p}{|G|^{1/6}} - x \right) \tag{4.125b}$$

$$q_{CHF,hq} = \frac{3.78 \times 10^3}{(D_h)^n |G|^{0.6}} h_p(1 - x) \tag{4.125c}$$

and

$$h_p = -1.159 + \frac{8.99\ P}{10 + P^2} + 0.149\ P \exp(-0.019\ P)$$

$$f_p = 0.7249 + 0.099\ P \exp(-0.032\ P)$$

$n = 0.4$ for $D_h \geq 1$ cm

$n = 0.6$ for $D_h < 1$ cm

D_h = hydraulic diameter (cm)

$|G|$ = absolute value of the mass flux (gm cm^{-2} s^{-1})

P = pressure (bar), and

x = equilibrium quality

Note that because the Biasi correlation uses cgs units, Eq. (4.125a) has a multiplication factor of 10^4 so that the units of q_{CHF} in IFCI will be W/m^2.

Typically, Eq. (4.125a) is the controlling correlation for low quality and Eq. (4.125b) for high quality. However, the value of the switch over quality is not constant and varies between about 0.3 and 0.7 depending upon the pressure.

Currently, IFCI uses the Biasi correlation for values of α_1 less than 0.97. For $0.97 < \alpha_1 < 0.98$, the code uses the value obtained at $\alpha_1 = 0.97$. For $\alpha_1 \geq 0.98$, T_{CHF} is fixed at 0.5 K above T_{sat}, the single phase liquid correlations explained in Section 4.2.1 are used. Also, because the Biasi correlation tends to overpredict the data at mass fluxes lower than 200 kg/(m^2s), the CHF for these conditions is evaluated by using the Biasi correlation with |G| = 200 kg/(m^2s).

Once q_{CHF} is obtained, the wall surface temperature corresponding to the CHF point, T_{CHF}, is calculated by using a Newton-Raphson iteration to determine the intersection of the heat flux found by using the nucleate-boiling HTC and the CHF. An iteration is required because $T_w = T_{CHF}$ must be known to evaluate the Chen correlation; and, in turn, the Chen HTC must be known to calculate the wall temperature, i.e.;

$$q_{CHF} = h_{CHF} (T_w - T_{sat}) . \tag{4.126}$$

The iteration equation for determining T_{CHF} can be expressed as

$$T_{CHF}^{n+1} = T_{CHF}^{n} - \frac{\left(T_{CHF}^{n} - T_{sat} - \frac{q_{CHF}}{h_{CHF}} \right)}{\left(1 + \frac{q_{CHF}}{h_{CHF}^2} \frac{dh_{CHF}}{dT_w} \right)} \tag{4.127}$$

where the superscript "n" is the iteration counter, h_{CHF} is the heat transfer coefficient evaluated by using the Chen correlation, and $\frac{dh_{CHF}}{dT_w}$ is the derivative of the heat transfer correlation with respect to the wall temperature. Currently, T_{CHF} is restricted to the range of

$$(T_{sat} + 0.5) \leq T_{CHF} \leq (T_{sat} + 100) \tag{4.128}$$

4.2.3.4.2 Assumptions and/or approximations

The CHF prediction in IFCI using the Biasi correlation is based upon the following assumptions:

1) The transient is slow enough that the CHF phenomenon is quasi-steady. This assumption allows the use of an empirical correlation based on steady-state data in order to model transient CHF.
2) CHF is only a function of the local thermal-hydraulic parameters and the history effects are negligible.
3) CHF is not affected by the flow direction. Using this assumption, the mass flux G in the original correlation is replaced by the absolute value of G in the code implementation.
4) The Biasi correlation was originally written for round tubes. In IFCI it is assumed that the tube diameter may be replaced by the flow channel hydraulic diameter.

4.2.3.4.3 Scaling Considerations

The Biasi correlation was developed for round tubes; however, Reference [26] suggests that its success in predicting the blowdown data in various tests indicates that it can be scaled to rod-bundle geometry using a hydraulic diameter. Its validity in other geometric regimes has not been examined.

4.2.3.4.4 Model as Coded

The application of these correlations within the code is straightforward. The actual coding can be found in subroutines CHFM, and CHF1M. We note that in Eq. (4.127) convergence is assumed if < 1.0, and maximum of ten iterations is allowed; if convergence does not occur, a message is printed and a fatal error occurs.

4.2.3.4.5 Assessment

The Biasi correlation is one of the more frequently referenced correlations in the literature. The results of a major assessment of this correlation were recently reported by Groeneveld et al. [27], in which the Biasi correlation was compared to approximately 15000 steady-state water data points that are stored in the Chalk River Nuclear Laboratories' CHF data bank. Also, Leung [28] has compared the Biasi correlation to transient CHF data. A review of these results and an assessment of the TRAC implementation has been given in Reference [5].

A summary of the assessment given in Reference [5] is as follows. The Biasi correlation yields reasonable results when compared to steady-state and transient annular flow dryout type CHF data. However, they note that the good comparison with the flow transient data was probably due to the fact that the data base being considered only had flow transients resulting in an annular flow regime prior to reaching CHF. Three areas of limitation or deficiency were

noted. First, the current approach cannot model subcooled or very low quality departure from nucleate boiling. Second, the predictions at low mass fluxes ($|G| < 200$ kg/(m^2s)) is an area in which there is very little information is available and further experimental CHF studies are required before confidence in the predictions can be obtained. Third, the high-void-fraction model needs further assessment even though it gives favorable results for rapid depressurization transients in which a sudden core voiding occurs.

Finally, they also note that one must be aware of the limitations imposed by the quasi-steady approach used. For example, applying the present model to rapid transients such as quenching, where the CHF prediction is needed to calculate the return to nucleate boiling while going from right to left on a typical boiling curve, may prove to be a problem.

4.2.3.5 Minimum Stable Film-Boiling Temperature

The minimum stable film-boiling temperature, T_{min}, is the intersection point between the transition- and film-boiling heat-transfer regimes. It is also used in the interpolation scheme for determining the transition-boiling heat flux.

4.2.3.5.1 Basis of the Model

In IFCI, the homogeneous-nucleation minimum stable film-boiling temperature correlation of Henry [29] is used. This approach was adopted directly from TRAC. This can be written as

$$T_{min} = T_{nh} + (T_{nh} - T_2)\sqrt{R} \tag{4.129a}$$

where

$$R = \frac{(k\rho C_p)_2}{(k\rho C_p)_w} \tag{4.129b}$$

and T_{nh} is the homogeneous-nucleation temperature. In Eq. (4.129b), the subscript 2 indicates liquid properties and the subscript w refers to wall properties. The homogeneous-nucleation temperature is calculated as

$$T_{nh} = 705.44 - (4.722 \times 10^{-2})DP + (2.3907 \times 10^{-5})DP^2 - (5.8193 \times 10^{-9})DP^3 \tag{4.130a}$$

where

$$DP = 3209.6 - P \tag{4.130a}$$

In Eq (4.130) the pressure P is in units of pounds per square inch atmospheric, and the temperature is in Fahrenheit units. In IFCI, the variable P is converted to a temporary variable in British units, and T_{nh} is converted to Kelvin after the equation is evaluated. We note that according to Ref. [5], Eq. (4.130) originated in the COBRA-TF code.

3.2.3.6.2 Assumptions and/or approximations

No additional assumptions need be mentioned here beyond those implied in the previous section.

3.2.3.6.3 Scaling Considerations

There are no parameters in the correlation to account for scaling geometry or mass flux. Fluid pressure, temperature, and thermal properties and wall thermal properties are the only parameters in the correlation; no limits are specified for these parameters.

3.2.3.6.4 Model as Coded

The application of this correlation within the code is straightforward. The actual coding can be found in subroutine TMSFBM. As mentioned above, since in Eq (4.130) the pressure P is in units of pounds per square inch atmospheric, and the temperature is in Fahrenheit units, a conversion needs to be made to make the units consistent. In IFC I, the variable P is converted to a temporary variable in British units, and then T_{nh} is converted to Kelvin after the equation is evaluated.

4.2.3.5.5 Assessment

In Ref. [5], a comparison of the predictions of this model to the data of Chen et al. [30], is made. Chen's experiment extends earlier work by Groeneveld and Steward [32] to separate the effects of axial conduction and hydraulic transients and is run over a short-enough test section in a steady-state manner such that these data, along with those of Groeneveld, represent the only known forced convective true T_{min} data. Because no additional assessment work has been down in the IFCI development effort, the reader is referred to Ref. [5] for the details of this comparison. In summary, a comparison of the TRAC (and thus IFCI) T_{min} model to true T_{min} data shows that the prediction is reasonable but could stand improvement in light of the more recent data. The prediction is called reasonable because the prediction is much closer to the data than are the apparent T_{min} values often developed from reflood and blowdown experiments. From the comparisons presented, it appears that the current T_{min} model

overpredicts the data at typical reflood conditions (0.1 to 0.4 MPa) by 100 to 150 K and underpredicts the data at typical blowdown conditions (7 MPa) by about 60 to 100 K.

4.2.3 Interpolation Regime

The interpolation region covers the temperature range $T_{sat} < T_3 < (T_{sat} + 5)$. This region has been defined so that the heat transfer values will behave smoothly as the flow conditions change from normal convection to boiling.

In this region, both the melt temperature T_3, and the normalized vapor volume fraction, α_v', are used as interpolation parameters. Over the interpolating temperature range, a linear interpolation scheme is used.

$$h_j = \left[\frac{(T_3 - T_{sat})}{5}\right] h_{j,boiling} + \left(1 - \left[\frac{(T_3 - T_{sat})}{5}\right]\right) h_{j,convection} \qquad (4.131)$$

where j refers to either vapor or water, and the coefficients $h_{1,convection}$ and $h_{1,boiling}$ are found as described in Sections 4.2.1 and 4.2.2 respectively.

For the vapor field, to interpolate over the region $0.75 \le \alpha_v' \le 0.98$, a cubic interpolating function (for which the derivatives are zero at the endpoints) is used.

$$h_1 = F1\, h_{1,boiling} + (1 - F1)\, h_{1,convection} \qquad (4.132)$$

where

$$F1 = (3 - 2x)\, x^2 \qquad (4.133)$$

$$x = \frac{(0.98 - \alpha_v')}{0.23}\,. \qquad (4.134)$$

For the water field, a series type interpolating function is used, i.e,

$$h_2 = \frac{1}{\frac{F1}{h_{2,boiling}} + \frac{(1-F1)}{h_{2,convection}}} \qquad (4.135)$$

5. REFERENCES

1. M. F. Young, IFCI: An Integrated Code for Calculation of All Phases of Fuel-Coolant Interactions, SAND87-1048, NUREG/CR- 5084, Sandia National Laboratories, Albuquerque, NM, 1987
2. M. F. Young, "Application of the IFCI Integrated Fuel-Coolant Interaction Code to a FITS-Type Pouring Mode Experiment," Dynamics of Detonations and Explosions : Explosion Phenomena, AIAA, Vol 134, 1990
3. F. J. Davis and M. F. Young, Integrated Fuel-Coolant Interaction (IFCI 6.0) Code User's Manual, NUREG/CR-6211, SAND94-0406, Sandia National Laboratories, Albuquerque, New Mexico, April 1994
4. Safety Code Development Group, TRAC-PF1/MOD1: An Advanced Best Estimate Computer Program for Pressurized Water Reactor Thermal-Hydraulic Analysis, NUREG/CR-3858, LA-10157-MS, Los Alamos National Laboratories, Los Alamos, NM, July 1986.
5. D. R. Liles, et. al. , TRAC-PF1/MOD1 Correlations and Models, NUREG/CR-5069, LA-11208-MS, R4, Los Alamos National Laboratories, Los Alamos, NM, 1988.
6. S. S. Dosanjh, Ed., MELPROG-PWR/MOD1: A Two Dimensional, Mechanistic Code for Analysis of Reactor Core Melt Progression and Vessel Attack Under Severe Accident Conditions, NUREG/CR-5193, SAND88-1824, Sandia National Laboratories, Albuquerque, NM, 1989.
7. R. C. Schmidt et al., MELPROG PWR/MOD1 Models and Correlations, SAND89-3123, NUREG/CR-5569, Sandia National Laboratories, Albuquerque, NM, 1992.
8. M. Ishii, Thermo-Fluid Dynamic Theory of Two-Phase Flow, Eyrolles, France, 1975
9. G. Kocamustafaogullari, Thermo-Fluid Dynamics of Separated Two-Phase Flow, Ph. D. dissertation, Georgia Inst. of Technology, Atlanta, GA, 1971.
10. J. H. Mahaffy, "A Stability-Enhancing Two-Step Method for Fluid Flow Calculations," J. Comp. Phys., Vol 46, p.329, 1982
11. W. R. Bohl et al., "Computational Methods of the Advanced Fluid Dynamics Model," Proc. ANS Mtg. on Advances in Reactor Physics, Mathematics, and Computation, Paris, France, 1987.
12. H. C. No and M. S. Kazimi, "Effect of Virtual Mass Effects on the Mathematical Characteristics and Numerical Stability of the Two-Fluid Model", Nucl. Sci. & Eng., Vol 89, pp.197-206, 1985.
13. O. Baker, "Design of Pipe Lines for Simultaneous Flow of Oil and Gas, " Oil and Gas Journal, 1954.
14. J. G. Collier, Convective Boiling and Condensation, McGraw-Hill, pp. 18-20, 1981.
15. G. B. Wallis, One Dimensional Two-Phase Flow, McGraw-Hill Book Company, New York, NY, 1969.
16. W. C. Rivard and M. D. Torrey, Numerical Calculation of Flashing from Long Pipes Using a Two-Field Model, LA-6104-MS, Los Alamos National Laboratory, Los Alamos, NM, November 1975.

17. B. B. Mikic, W. M. Rohsenow, and P. Griffith, "On Bubble Growth Rates," Int. J. Heat and Mass Transfer, 13, 657-666, 1970.
18. K. Lee and D. J. Ryley, "The Evaporation of Water Droplets in Superheated Steam," ASME paper 68-HT-11, 1968.
19. Hinze, "Fundamentals of the Hydrodynamic Mechnism of Splitting in Dispersion Processes," AIChE J., Vol 1 (3), pg 289-295, 1955.
20. R. B. Bird, W.E. Stewart, and E.N. Lightfoot, Transport Phenomena, John Wiley and Sons, Inc., New York, NY, 1960.
21. J. C. Chen, "A Correlation for Boiling Heat Transfer of Saturated Fluids in Convective Flow," ASME paper 63-HT-34, 1963.
22. H. K. Forster and N. Zuber, "Bubble Dynamics and Boiling Heat Transfer," AIChE J., 1, 532-535, 1955.
23. V. K. Dhir and G. P. Purhoit, "Subcooled Film-Boiling Heat Transfer from Spheres," Nuclear Engineering and Design, Vol 47, pp. 49-66, 1978.
24. L. A. Bromley, N. R. LeRoy, and J. A. Robbers, "Heat Transfer in Forced Convection Film Boiling," Ind. and Engng. Chem., Vol 45, pp.2639-2646, 1953.
25. L. Biasi, G.C. Clerici, S. Garribba, R. Sala, and A. Tozzi, "Studies on Burnout, Part 3: A New Correlation for Round Ducts and Uniform Heating and Its Comparison with World Data," Energia Nucleare, 14, 530-536, 1967.
26. W. M. Rohsenow and H. Y. Choi, Heat, Mass, and Momentum Transfer, Prentice-Hall Inc., Englewood Cliffs, NJ, 1961.
27. D. C. Groeneveld, S.C. Cheng, and T. Doan, "1986 AECL-UO Critical Heat Flux Lookup Table," Heat Transfer Engineering, 7, 46-62, 1986.
28. J. C. M. Leung, Transient Critical Heat Flux and Blowdown Heat Transfer Studies, Ph.D. Dissertation, Northwestern University, June 1980.
29. R. E. Henry, "A Correlation for the Minimum Flim Boiling Temperature," AIChE Symposium Series, 138, 81-90, 1974.
30. S. C. Cheng, P. W. K. Law, and K. T. Poon, "Measurements of True Quench Temperature of Subcooled Water Under Forced Convection Conditions," Int. J. of Heat and Mass Transfer, 20(1), 235-243, 1985.
31. D. C. Groeneveld and J. C. Stewart, "Measurement of Axially Varying Nonequilibrium in Post-Critical-Heat-Flux Boiling in a Vertical Tube," Lehigh University, NUREG/CR-3363, June 1983.